



Research Article

Open Access

## Synthesis of titanium dioxide-polyoxometalate nanocomposite films supported on indium tin oxide plates by electrodeposition for photocatalytic decolourization of dyes

S. Clara Anthoniamma and, H. Gurumallesh Prabu

Department of Industrial Chemistry, School of Chemical Sciences, Alagappa University, Karaikudi-630 003, Tamilnadu, India.

Received: July 02, 2015 / Accepted: July 10, 2015  
© Science Research Library

### Graphical Abstract



### Abstract

Copper hetero poly acid and tungsten hetero poly acid compounds were used as model polyoxometalates. Sol was prepared using polyoxometalate and TiO<sub>2</sub> derived from titanium tetraisopropoxide. This sol was electrodeposited on indium tin oxide (ITO) plate. The TiO<sub>2</sub>-polyoxometalate nanocomposite was formed on the surface of ITO as film. The film thus obtained was characterized by XRD, FT-IR, SEM, UV-DRS, AFM and PL analyses. XRD results indicate the presence of TiO<sub>2</sub> and polyoxometalate in the nanocomposite film. FT-IR results show the existence of metal-oxygen-metal linkage in the composite. Narrow band gap noticed from UV-DRS spectra reveals the interaction of POM with TiO<sub>2</sub>. The nanocomposite film was tested for photocatalytic activity in the decolourization of model pollutant dyes such as Reactive Red 2 (RR2) and Disperse Yellow 231 (DY231). The decolourization efficiency and reusability of tungsten based composite film was higher than that of copper based composite film.

Keywords: TiO<sub>2</sub>, polyoxometalates, electrodeposition, ITO, photocatalytic.

### Introduction

TiO<sub>2</sub> is an excellent candidate for a broad range of applications due to its physicochemical properties, wide band gap semiconductor, low-cost, abundant and a relatively nontoxic nature. TiO<sub>2</sub> enhances the catalytic activity of a system due to strong interactions between the active phase and the TiO<sub>2</sub> support. Among the three phases of TiO<sub>2</sub>, anatase phase exhibits tremendous attention for potential applications in paints and photodegradation of environmentally toxic dyes and organic pollutants. Pearson et al. (2013). The application of TiO<sub>2</sub> particles is limited due to the large band gap and charge recombination (or electron-hole recombination), whereby an inherently large driving force promotes the recombination of electron and the newly generated hole upon photo excitation that reduces its overall photocatalytic performance. Effort has been put forward to shift the band gap energy of TiO<sub>2</sub> particles toward the visible region of the spectrum, where photoexcitation can become more energetically favourable. Lu et al. (2012).

Polyoxometalates (POMs), a well-known class of inorganic clusters with a metal-oxygen framework, have an intrinsic ability to accept electrons readily Ozer et al. (2001) Tachikawa et al. (2006). POMs can successively transfer the photogenerated electrons from the TiO<sub>2</sub> conduction band to the empty d orbit, thus greatly improving the photoactivity of composite due to the synergistic effect of POMs and TiO<sub>2</sub>. Some POMs supported on TiO<sub>2</sub> composite materials as heterogeneous photocatalysts exhibit relatively higher photocatalytic degradation abilities towards aqueous organic pollutants. Studies on photocatalysts are mainly based on powders that severely hindered the practical applications due to the post-treatment problems such as separation, recovery and reuse. To overcome these disadvantages, much attention has been paid to explore immobilized TiO<sub>2</sub>-based film materials. Niu et al. (2013).

Dye molecules are extensively used in textile dyeing, paper printing, leather, pharmaceutical, cosmetic and nutrition industries. Textile industries generate wastewaters that contain considerable

Corresponding author: [hgprabu2010@gmail.com](mailto:hgprabu2010@gmail.com)

amounts of non-fixed dyes and a huge amount of inorganic salts. Principal sources of environmental aqueous contamination in wastewaters are dyes. They need to be removed from wastewaters by different methods. The most often used methods for the treatment of textile dyes, including membrane filtration, adsorption, biological degradation, ozonation are not efficient enough. Advanced oxidation processes (AOPs) seem to be a very promising way to deal with the problem of organic pollutants destruction in aqueous systems. Among the AOPs, heterogeneous photocatalysis was found as an emerging destructive technology leading to the total mineralization of most organic pollutants. Behnajady et al. (2011).

Electrodeposition is a promising technique for the preparation of transparent nanocrystalline semiconductor oxide thin films in large area substrates. Electrodeposition process from an aqueous solution is cost effective, environmentally friendly and advantageous to achieve facile control of the film thickness. Tangestaninejada et al. (2010).

In this research work copper based heteropolyacid and tungsten based heteropolyacid were used as model polyoxometalates. Sol was prepared using polyoxometalate and  $\text{TiO}_2$  derived from titanium tetraisopropoxide (TTIP) and electrodeposited on indium tin oxide (ITO) plate. Reactive Red 2 (RR2) and Disperse Yellow 231 (DY231) dyes were used as model pollutants.

Preparation of  $\text{TiO}_2$ -POM nanocomposite film on ITO, characterization of film by analytical techniques and photocatalytic activity of the film in the decolorization of dyes are studied and presented.

## Materials and methods

Titanium tetraisopropoxide 99.5% was purchased from Aldrich and used as such. Copper based (designated as P1) and tungsten based (designated as P2) polyoxometalates were synthesized as per procedures outlined and kindly supplied by Dr. Monika Goral of Poland. Purified water was obtained using TKA-LAB Reinst water system.

## Synthesis of $\text{TiO}_2$ -POM sol

$\text{TiO}_2$  sol was prepared using TTIP, P1 or P2 and nitric acid. The preparation of film was performed in three steps; (1) synthesis of composite sol, (2) electrodeposition of sol on ITO plate and (3) annealing. For step 1, 1 mL of TTIP was slowly dropped into 20 mL of 0.5 M nitric acid and stirred vigorously for 2 h at  $70^\circ\text{C}$ . To this, 0.6 g of POM (either P1 or P2) was added and stirred on a magnetic stirrer for 1 h at  $70^\circ\text{C}$ .

## Coating of the sol on ITO plates

In step 2, electrodeposition was performed using CHI-620A instrument with a three electrode setup. Prior to the electrodeposition, the ITO plate was thoroughly cleaned with acetone and kept in an oven at  $100^\circ\text{C}$  for 15 min. Cleaned ITO plate as the working electrode, platinum wire as the counter electrode and Ag/AgCl as the reference electrode were used in the 3 electrode set up. The coating solution consisted of 10 ml sol and 1 ml acetate buffer (pH 1) solution. Anodic electrodeposition was carried out on the ITO electrode at a potential application of 1.0 V for 30 min. After the deposition, the composite film thus formed

was washed with distilled water and dried at  $100^\circ\text{C}$  for 10 min. The ITO plate containing the composite film was annealed at  $400^\circ\text{C}$  for 2 h. The composite film thus obtained with copper based was designated as P<sub>1</sub>T and with tungsten based was designated as P<sub>2</sub>T.

## Characterization

The films were subjected to characterization. UV-Vis diffuse reflection spectra (DRS) were obtained using Shimadzu UV-3101PC spectrophotometer equipped with an integrating sphere and  $\text{BaSO}_4$  as a reference. Fourier transform infrared (FT-IR) spectra were obtained using Shimadzu 8400S spectrophotometer. Photoluminescence (PL) spectra of the samples were obtained using FluoroMax-3, Jobin-Yvon-Horiba PL system in the study range from 300 to 900 nm using excitation line at  $\lambda$  300 nm. X-ray diffraction (XRD) measurements were performed using X'Pert-PRO diffractometer with Cu K radiation. Leo series 1430 VP equipped with INCA instrument was used to record scanning electron microscopy (SEM) image of samples. The surface roughness of film was studied by atomic force microscopy (AFM) at tapping mode with a Nanoscope III Digital-VEECO (E type scanner,  $512 \times 512$  pixels, with scanned size  $500 \text{ nm} \times 500 \text{ nm}$ ).

## Photocatalytic activity

The photocatalytic activity of P<sub>1</sub>T and P<sub>2</sub>T films was studied with the aqueous solutions of RR2 and DY231 dyes at a concentration of  $10^{-4}$  mol L<sup>-1</sup>. Warm soft lamp (visible) having wavelength greater than 370 nm and color temperature of 3000 K was used as photo source. The photocatalytic decolorization efficiency of P<sub>1</sub>T and P<sub>2</sub>T films was tested using UV-vis spectral absorbance of the dye solution before and after the activity. Effect of pH was studied at different conditions such as 1, 7 and 13.

## Results and discussion

### XRD analysis

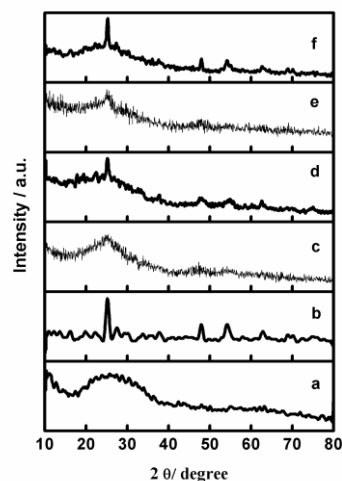


**Figure.1.** XRD patterns of a) as deposited  $\text{TiO}_2$  film b) annealed  $\text{TiO}_2$  film c) as deposited P<sub>1</sub>T film d) annealed P<sub>1</sub>T film e) as deposited P<sub>2</sub>T film f) annealed P<sub>2</sub>T film

The XRD patterns obtained for as deposited  $\text{TiO}_2$ , P<sub>1</sub>T, P<sub>2</sub>T films and annealed  $\text{TiO}_2$ , P<sub>1</sub>T, P<sub>2</sub>T composite films are shown in Fig.1. As deposited  $\text{TiO}_2$  and P<sub>1</sub>T composite films are found to

be amorphous in nature, but the as deposited P<sub>2</sub>T film shows improved crystallinity. This is evidenced from the peak at 25° usually observed for anatase. Annealed TiO<sub>2</sub> film exhibits anatase phase since diffraction peaks are observed at 25.3°, 37.8°, 48.0°, 54.4°, and 62.7°. Similar characteristic peaks are observed for the annealed P<sub>1</sub>T and P<sub>2</sub>T composite films, which reveal the formation of anatase phase. An additional less intense peak is observed at 35° for P<sub>2</sub>T. It is reported that the diffractions originated from the interaction between Keggin unit and TiO<sub>2</sub> are hardly observed for the composites containing polyoxometalates. Lu et al. (2012). This may be due to the interaction of phosphotungstate in the octahedral interstitial site or the substitutional position of TiO<sub>2</sub>. These results infer that the phosphotungstate might interact with titania through oxygen atom at the corner of Keggin structure. Tangestaninejada et al. (2010). Ullah et al. (2013). From the difference in XRD peak intensity at 25°, 48° and 54°, it is inferred that the electrodeposition on ITO plate resulted into the formation of TiO<sub>2</sub>-polyoxometalate composites (P<sub>1</sub>T and P<sub>2</sub>T) effectively.

### FT-IR analysis

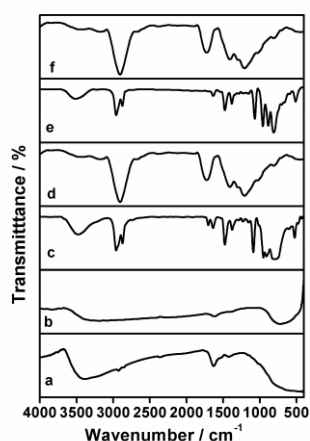


**Figure.2** FT-IR spectra of a) as deposited TiO<sub>2</sub> film b) annealed TiO<sub>2</sub> film c) as deposited P<sub>1</sub>T film d) annealed P<sub>1</sub>T film e) as deposited P<sub>2</sub>T film f) annealed P<sub>2</sub>T film

FT-IR spectra of as deposited and annealed TiO<sub>2</sub>, P<sub>1</sub>T and P<sub>2</sub>T films are shown in Fig.2. The absorption peak observed at 1632 cm<sup>-1</sup> for as deposited TiO<sub>2</sub> may be attributed to the bending vibration of free O-H bond or the stretching mode of Ti-OH. Tayade et al. (2007). Similar less intense peak is observed at 1640 cm<sup>-1</sup> for as deposited P<sub>1</sub>T and P<sub>2</sub>T. The band observed at 3399 cm<sup>-1</sup> for as deposited TiO<sub>2</sub> film is attributed to the OH stretching of surface absorbed water. In the annealed TiO<sub>2</sub> film, the intensity of OH stretching at 3399 cm<sup>-1</sup> has been considerably reduced due to the heat treatment. The peaks observed for as deposited P<sub>1</sub>T film at 3476 cm<sup>-1</sup> and for as deposited P<sub>2</sub>T film at 3500 cm<sup>-1</sup> are attributed to OH stretching vibration. In the annealed P<sub>1</sub>T and P<sub>2</sub>T films, the intensity of OH stretching at 3476 cm<sup>-1</sup> has been considerably reduced upon calcination. Absorption peaks noticed at 2960 cm<sup>-1</sup> and 2872 cm<sup>-1</sup> for as deposited P<sub>1</sub>T and P<sub>2</sub>T film attributes to the N-H stretching vibrations. The peaks observed at 1092 cm<sup>-1</sup>, 932 cm<sup>-1</sup>

and 790 cm<sup>-1</sup> for as deposited P<sub>1</sub>T attributes to laccunary keggin type structure. The characteristic bands noticed in the region from 1100 to 700 cm<sup>-1</sup> for as deposited P<sub>2</sub>T film are attributed to the possible vibrations between W-O and W-O-W. Yang et al. (2003). The peak observed at 536 cm<sup>-1</sup> for the as deposited P<sub>1</sub>T and P<sub>2</sub>T film has been widened in the annealed P<sub>1</sub>T and P<sub>2</sub>T film. This shows that strong interactions were built between anions of polyoxometalates and TiO<sub>2</sub>. The hydrolysis of TTIP has resulted in titanium hydroxide (Ti-OH) containing products. In these products, the Ti atoms in Ti-OH groups are assumed to contain electrophilic properties. In the case of P<sub>2</sub>T, Ti-OH groups were chemically linked to the surface of POM via W-O-Ti bonds, resulting in the saturation of the surface oxygen atoms of XW11 clusters. From the spectra it is noticed that both as deposited P<sub>1</sub>T and P<sub>2</sub>T films had almost similar interactions with variations in intensity. This has been reflected in the case of P<sub>1</sub>T and P<sub>2</sub>T annealed composite films. The shift in peak position and intensity between as deposited and annealed films confirm the formation of composite with strong interaction between polyoxometalate and TiO<sub>2</sub>.

### SEM analysis

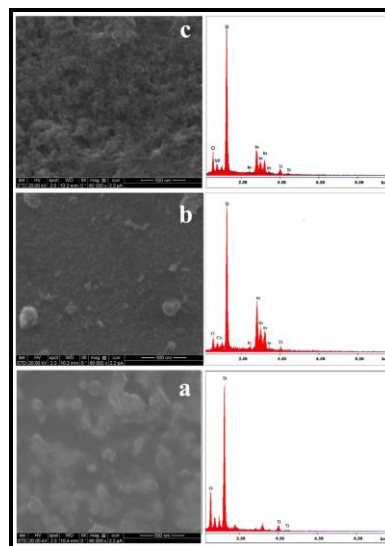


**Figure.3.** SEM images of a) annealed TiO<sub>2</sub> film b) annealed P<sub>1</sub>T film c) annealed P<sub>2</sub>T film

The SEM images of the annealed TiO<sub>2</sub>, P<sub>1</sub>T and P<sub>2</sub>T films are shown in Fig.3. The SEM image of P<sub>1</sub>T has a few localised aggregation with smooth and homogenous surface. The energy dispersive spectrum (EDX) results reveal the presence of titanium, oxygen and copper. These results confirm the formation of P<sub>1</sub>T composite. The SEM image of P<sub>2</sub>T shows uniform film formation with some gutters. The film surface is relatively smooth over a large area. This might be due to the deposition of polyanions of tungsten on ITO plates. Liu et al. (2009). The EDX spectrum of the sample has revealed the presence of titanium, tungsten and oxygen in P<sub>2</sub>T film. These results indicate that the morphology of TiO<sub>2</sub> in P<sub>1</sub>T and P<sub>2</sub>T composite films are different for different materials.

**AFM analysis**

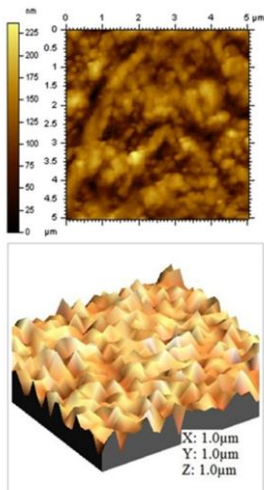


**Figure.4** AFM images of annealed TiO<sub>2</sub> film

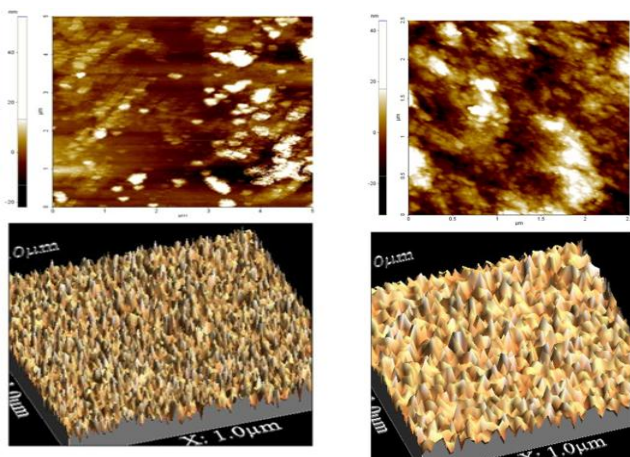
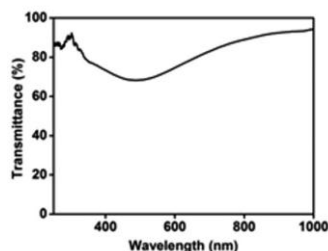


**Fig.5** AFM images of annealed P<sub>1</sub>T film

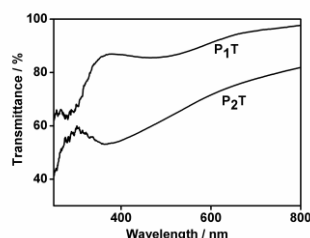
**Fig.5** AFM images of annealed P<sub>2</sub>T film

Fig.4 shows the AFM images of the annealed TiO<sub>2</sub> films. The surface roughness of the annealed TiO<sub>2</sub> films is 0.2834 μm. AFM image of the P<sub>1</sub>T film is shown in Fig.5. The two-dimensional and three-dimensional images provide detailed information about the surface morphology and roughness of nanocomposite films. Granular pattern of arrangement is observed from the images. As the POM polyanions can reduce the coulombic repulsion of adjacent positive TiO<sub>2</sub> nanoparticles, the aggregation of TiO<sub>2</sub> colloidal nanoparticles may occur to a certain level. The average roughness of the film is calculated as 0.2515 μm. The topography of the composite films suggests the interactions between TiO<sub>2</sub> and P<sub>1</sub> and the fine dispersion of POM particles in TiO<sub>2</sub> inorganic network. The formation of films by electrodeposition could be considered as evidence in the interaction between P<sub>1</sub> and TiO<sub>2</sub>. Fig.6 shows the AFM image of P<sub>2</sub>T film. The average surface roughness of the film is calculated as 0.2532 μm. The morphological changes of P<sub>1</sub>T or P<sub>2</sub>T composite films with that of the pristine TiO<sub>2</sub> film might be due to varied interactions between the two components. He et al. (2009).

**UV-DRS analysis**



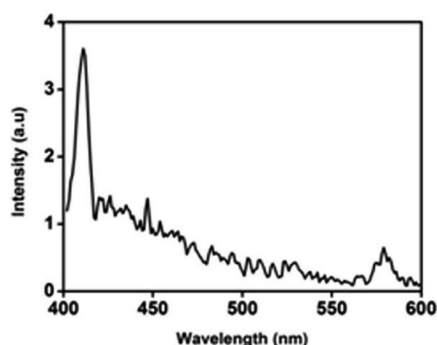
**Fig.7** UV-DRS spectra of annealed TiO<sub>2</sub> film



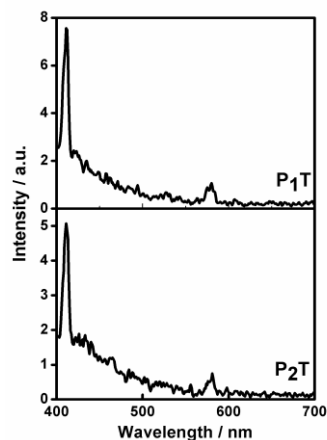
**Fig.8** UV-DRS spectra of annealed P<sub>1</sub>T film and annealed P<sub>2</sub>T film

Fig.7 shows UV- DRS spectra of annealed TiO<sub>2</sub> film. The calculated band gap of annealed TiO<sub>2</sub> film is 1.8 eV which is smaller than reported value 3.2 eV. Fig.8 shows UV- DRS spectra of P<sub>1</sub>T and P<sub>2</sub>T films. The results show the interaction between the primary Keggin structure and TiO<sub>2</sub> nanostructure that depend on the type of polyoxometalate. This may be due to the changes in coordination environment of TiO<sub>2</sub>. Tangestaninejada et al. (2010). Ullah et al. (2013). The bandgap energy (E<sub>g</sub>) of the P<sub>1</sub>T composite film calculated through Kubelka-Munk formula is 3.1 eV. The bandgap energy (E<sub>g</sub>) calculated for the P<sub>2</sub>T composite film is 2.3 eV. The widening of the band gap in the composite films may be due to the interaction of Keggin unit with TiO<sub>2</sub>. The charge transfer occurs from O (2p) to Ti (3d) orbit in pristine TiO<sub>2</sub> film. But in the case of composite films, the charge transfer occurs from O (2p) to the new conduction band that is constructed from the hybridization of Ti (3d) and W (5d) orbit. Lu et al. (2012). The changes in the coordination environment of Ti may be due to the interaction of polyoxometalates with TiO<sub>2</sub>. The transmittance edges of the composite films continuously extended to the longer wavelength.

**Photoluminescence analysis**



**Fig.9** Photoluminescence spectrum of annealed TiO<sub>2</sub> film.



**Fig.10** Photoluminescence spectra of annealed P<sub>1</sub>T and P<sub>2</sub>T films

The PL spectrum of annealed TiO<sub>2</sub> film is shown in Fig.9. The photoluminescence spectra show different patterns for different POM-TiO<sub>2</sub> composites (Fig.10). A peak is observed at 580 nm for TiO<sub>2</sub>, P<sub>1</sub>T and P<sub>2</sub>T films. This peak is attributed to the electronic transition mediated by the defect levels such as oxygen vacancies in the band gap. The emission peak observed at 412 nm for both P<sub>1</sub>T and P<sub>2</sub>T corresponds to the TiO<sub>2</sub> nanoparticles. Kulak et al. (2009). The tiny peaks observed in the range from 420 nm to 560 nm for P<sub>1</sub>T and P<sub>2</sub>T films may be due to the excitonic photoluminescence trapped by surface states and defects. Liu et al. (2007). The increased photoluminescence intensity observed in P<sub>1</sub>T than in P<sub>2</sub>T indicates the lower crystallinity of P<sub>1</sub>T film. Fang et al. (2008).

**Photocatalytic Activity**

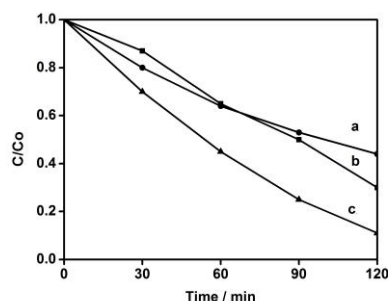


**Fig.11** Photocatalytic activity of a) annealed TiO<sub>2</sub> film b) P<sub>1</sub>T and c) P<sub>2</sub>T films in the decolorization of RR2 dye

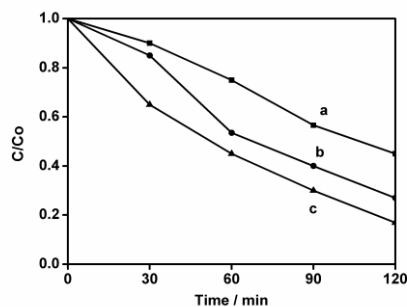


**Fig.12** Photocatalytic activity of a) annealed TiO<sub>2</sub> film b) P<sub>1</sub>T and c) P<sub>2</sub>T films in the decolorization of DY231 dye

Photocatalytic experiments were carried out to evaluate the effectiveness of the annealed TiO<sub>2</sub> and POM-TiO<sub>2</sub> composite films for the decolorization of azo dyes that are the major contaminant in textile wastewater. The decolorization efficiency using P<sub>1</sub>T film in 2 h of irradiation time was found to be 75% and 56% for RR2 and DY231 dyes respectively; but at similar experimental conditions, the decolorization efficiency of P<sub>2</sub>T film was found to be 83% and 81% for RR2 and DY231 dyes respectively. This clearly shows that the photocatalytic activity of P<sub>2</sub>T is higher than P<sub>1</sub>T. The rate of photocatalytic decolorisation is not only affected by the nature of film, but also by the transport of species (dyes) to and from bulk solution. The degradation curves of RR2 dye are slightly shifted to a lower C/Co value than the values of DY231 (fig.11 and fig.12). Improved photocatalytic activity of P<sub>1</sub>T and P<sub>2</sub>T composite film is mainly attributed to the existing interaction between TiO<sub>2</sub> and Keggin unit which results in the retardation of the recombination of the photoexcited hole and electron pairs owing to trapping photoexcited electrons into unoccupied metal 5d states of Keggin unit. Lu et al. (2012). From the rate constant values obtained, it is noted that P<sub>2</sub>T film shows improved efficiency for DY231 dye than RR2 dye. It is clear from the R<sup>2</sup> values (Table.1) that all reactions follow more or less pseudo first-order kinetics. The higher surface area in the composite also provides a higher number of catalytic sites on the surface of TiO<sub>2</sub> with less recombination of electron hole pairs, which is the rate-determining step in the photocatalytic degradation. The improved photocatalytic activity of P<sub>2</sub>T film may be due to its increased surface area, good porosity, presence of hydroxyl group and lowered band gap energy. It is reported that reduced band gap retards the charge recombination ratio that advantages for the photocatalytic performance. Peerakiathajorn et al. (2012). Amines and hydroxyl groups are very strongly active ortho and para directors with non-bonding electrons. Generally these electron donating substituent groups inductively take electrons from the ring and give it back by resonance. Hence, the decolorisation of the dyes strongly depends on the chemical structure and substituent groups. In RR2, two sulphonic acid groups are present, which are electron withdrawing favouring reduction. Both the dyes contain hydroxyl group conjugated with azo group that usually exists an equilibrium mixture of two tautomeric forms (azo or hydrazone) in the aqueous solution. It is reported that when the hydroxyl group is positioned in a naphthol, ortho to the azo bond, the hydrazone form is favourable at equilibrium. Hence intramolecular hydrogen bonding could be formed in the solution. Yu et al. (2004).

**Table.1** Calculated Rate constant values for the two composite films

| Composite        | RR2 dye        |        | DY231 dye      |        |
|------------------|----------------|--------|----------------|--------|
|                  | R <sup>2</sup> | K      | R <sup>2</sup> | k      |
| TiO <sub>2</sub> | 0.997          | 0.008  | 0.981          | 0.006  |
| P <sub>1</sub> T | 0.983          | 0.0230 | 0.966          | 0.0230 |
| P <sub>2</sub> T | 0.988          | 0.0460 | 0.986          | 0.0276 |

### Reusability of the film

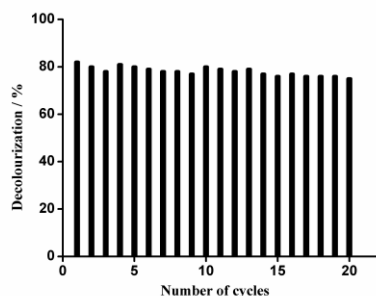


Fig.13 Photocatalytic efficiency of P2T film on reuse

Between the composite films, P<sub>2</sub>T film showed improved performance than P<sub>1</sub>T film in the photocatalytic decolourization of dyes. Thus, P<sub>2</sub>T film was chosen to evaluate the reusability, which is particularly important in the practical applications. This composite film was used for twenty photocatalytic cycles with RR2 dye solution. After each cycle, the film was washed with distilled water, dried in air and reused under the same photocatalytic conditions (10 ml of 0.4 M dye, pH 1). Fig.13 shows the performance of P<sub>2</sub>T film with good decolourization efficiency at an average about 80%. The reusability results indicated that the film was sufficiently active even up to 20 cycles.

### Conclusions

Annealed TiO<sub>2</sub> and TiO<sub>2</sub>-POM composite films were prepared by sol-gel method followed by electrodeposition process onto ITO plates. The structure and morphology of the films were characterised by XRD, FT-IR, SEM, UV-DRS, AFM and PL techniques. Changes in XRD patterns and shifts in peak position noticed from FT-IR spectra between as deposited and annealed films evidenced the formation of TiO<sub>2</sub>-POM composite films. SEM and AFM images also support the formation of TiO<sub>2</sub>-POM composite films. Narrowed band gap was observed for P<sub>1</sub>T and P<sub>2</sub>T composite films. The photoluminescence spectral peaks reveal the strong interaction between TiO<sub>2</sub> and polyoxometalates. The photocatalytic decolourization of RR2 and DY231 dyes in aqueous solution was evaluated using the annealed TiO<sub>2</sub> and composite films. P<sub>2</sub>T composite film showed improved activity than P<sub>1</sub>T due to the synergistic effect existed between P<sub>2</sub> and TiO<sub>2</sub>. P<sub>2</sub>T film was tested for reusability up to 20 cycles and found to be active.

### Acknowledgements

The authors wish to thank DST-PURSE, UGC project (34372/2008) for the provision of research facilities. The provision of XRD facility by the Department of Physics, Alagappa University is greatly acknowledged.

### References

- Behnajady, M. A., Eskandarloo, H., Modirshahla N., Shokri, M. (2011). Influence of the chemical structure of organic pollutants on photocatalytic activity of TiO<sub>2</sub> nanoparticles: kinetic analysis and evaluation of electrical energy per order (EEO). *Digest Journal of Nanomaterials and Biostructures*. 6, 1887-1895.
- Abdel-Rahman, R.M., Abdel-Mohsen, A.M., Moustafa, M.G.F., Salem, S.A.D., Mohame, A.S., El-Shamy, I.E. (2013). Finishing of cellulosic fabrics with Chitosan/polyethylene glycol-siloxane to improve their Performance and antibacterial properties. *Life Sci J*. 10, 834-839.
- Fang, D., Huang, K., Liu, S., Huang, J. (2008). Fabrication and Photoluminescent Properties of Titanium Oxide Nanotube Arrays. *J. Braz. Chem. Soc.* 19, 1059-1064.
- He, Q., Yan, L., Wei, F., YiMin, Z. (2009). Structure and photochromic properties of molybdenum phosphoric acid/TiO<sub>2</sub> composite films. *Science China Series B-Chem.*, 52, 169-173.
- Kulak, A., Kokorin, A., Kulak, T., Meissner, D. (2009). Molecular scale organized polyconjugated polymer-heteropolyacid composites. *Proceedings of the Estonian Academy of Sciences*. 58, 12-17.
- Liu, B., Wen L., Zhao, X. (2007). The photoluminescence spectroscopic study of anatase TiO<sub>2</sub> prepared by magnetron sputtering. *Materials Chemistry and Physics*. 106, 350-353.
- Liu, S., Xu, L., Gao, G., Xu, B., Guo, W. (2009). Electrochromic multilayer films with enhanced stability based on polyoxometalate and TiO<sub>2</sub>. *Materials Chemistry and Physics*. 116, 88-93.
- Kavkler, K., Demsar, A. (2011). Examination of cellulose textile fibres in historical objects by micro-Raman spectroscopy. *Spectrochim Acta A*. 78, 740-746.
- Lu, N., Zhao, Y., Liu, H., Guo, Y., Yuan, X., Xu, H., Peng H., Qin, H. (2012). Design of polyoxometalate-titania composite film (H<sub>3</sub>PW<sub>12</sub>O<sub>40</sub>/TiO<sub>2</sub>) for the degradation of an aqueous dye Rhodamine B under the simulated sunlight irradiation. *Journal of Hazardous Materials*. 199, 1-8.
- Niu, P., Hao, J. (2013). Photocatalytic degradation of methyl orange by titanium dioxide-decatungstate nanocomposite films supported on glass slides. *Colloids and Surfaces A: Physicochemical Engineering Aspects*. 431, 127-132.
- Ozer, R.R., Ferry, J.L. (2001). Investigation of the Photocatalytic Activity of TiO<sub>2</sub>-Polyoxometalate Systems. *Environ. Sci. Technol*. 35, 3242-3246.
- Pearson, A., Bhosale, S., Bhargava, S.K., Bansal, V. (2013). Combining the UV-Switchability of Keggin Ions with a Galvanic Replacement Process to Fabricate TiO<sub>2</sub>-Polyoxometalate-Bimetal Nanocomposites for Improved Surface Enhanced Raman Scattering and

- Solar Light Photocatalysis. *Appl. Mater. Interfaces.* 5, 7007-7013.
- Peerakiatkhajorn, P., Chawengkijwanich, C., Onreabroy, W., Chiarakorn, S. (2012). Novel Photocatalytic Ag/TiO<sub>2</sub> Thin Film on Polyvinyl Chloride for Gaseous BTEX Treatment. *Materials Science Forum.* 712, 133-145.
- Tachikawa, T., Tojo, S., Fujitsuka M., Majima, T. (2006). One-Electron Redox Processes during Polyoxometalate-Mediated Photocatalytic Reactions of TiO<sub>2</sub> Studied by Two-Color Two-Laser Flash Photolysis. *Chem. Eur. J.* 12, 3124-3131.
- Tangestaninejada, S., Moghadama, M., Mirkhania, V., Baltorka I. M., Salavatic, H. (2010). Vanadium-containing polyphosphomolybdate immobilized on TiO<sub>2</sub> nanoparticles: A recoverable and efficient catalyst for Photochemical, Sonochemical and photosonochemical degradation of dyes under irradiation of UV light. *J. Iranian Chemical Society.* 7, S161- S174.
- Tayade, R. J., Surolia, P. K., Kulkarni R. G., Jasra, R.V. (2007). Photocatalytic degradation of dyes and organic contaminants in water using nanocrystalline anatase and rutile TiO<sub>2</sub>. *Science and Technology of Advanced Materials.* 8, 455-462.
- Ullah, S., Acuna, J.J.S., Pasa, A. A. S., Bilmes, A. Vela, M. E., Benitez, G., Filho, U. P. R. (2013). Photoactive layer-by-layer films of cellulose phosphate and titanium dioxide containing phosphotungstic acid. *Applied Surface Science.* 277, 111-120.
- Yang, Y., Guo, Y., Hu, C., Jiang C., Wang, E. (2003). Synergistic effect of Keggin-type [X<sub>n</sub>+W<sub>11</sub>O<sub>39</sub>](12-n)- and TiO<sub>2</sub> in macroporous hybrid materials [X<sub>n</sub>+W<sub>11</sub>O<sub>39</sub>](12-n)-TiO<sub>2</sub> for the photocatalytic degradation of textile dyes. *J. Mater. Chem.* 13, 1686-1694.
- Yu, J., Jia J., Ma, Z. (2004). Comparison of Electrochemical Behavior of Hydroxyl-substituted and Nonhydroxyl-substituted Azo Dyes at a Glassy Carbon Electrode. *Journal of Chinese Chemical Society.* 51, 1319-1324.



Science Research Library (SRL) Open Access Policy

SRL publishes all its journals in full open access policy, enables to access all published articles visible and accessible to scientific community.

SRL publishes all its articles under Creative Commons Attribution - Non-Commercial 4.0 International License



Authors/contributors are responsible for originality, contents, correct references, and ethical issues.

Author benefits:

- ✓ Online automated paper status
- ✓ Quality and high standards of peer review
- ✓ Rapid publication
- ✓ Open Access Journal Database for high visibility and promotion of your research work
- ✓ Inclusion in all major bibliographic databases
- ✓ Access articles for free of charge